THE JOURNAL OF BIOLOGICAL CHEMISTRY
Vol. 278, No. 43, Issue of October 24, pp. 42121–42130, 2003

Printed in U.S.A.

A3 Adenosine Receptor Activation in Melanoma Cells

ASSOCIATION BETWEEN RECEPTOR FATE AND TUMOR GROWTH INHIBITION*

Received for publication, February 5, 2003, and in revised form, July 15, 2003
Published, JBC Papers in Press, July 15, 2003, DOI 10.1074/jbc.M301243200

Lea Madi‡, Sara Bar-Yehuda‡§, Faina Barer‡, Eti Ardon‡, Avivit Ochaion‡, and Pnina Fishman‡§¶

From the ‡Can-Fite BioPharma Ltd., Kiryat-Matalon, Petach-Tikva, 49170 and the §Laboratory of Clinical and Tumor Immunology, The Felsenstein Medical Research Center, Tel-Aviv University Sackler Faculty of Medicine, Rabin Medical Center, Petach-Tikva 49100, Israel

Activation of the G_i protein-coupled A3 adenosine receptor (A3AR) has been implicated in the inhibition of melanoma cell growth by deregulating protein kinase A and key components of the Wnt signaling pathway. Receptor activation results in internalization/recycling events that play an important role in turning on/off receptor-mediated signal transduction pathways. Thus, we hereby examined the association between receptor fate, receptor functionality, and tumor growth inhibition upon activation with the agonist 1-deoxy-1-[6-[[(3-iodophenyl)-methyl]amino]-9*H*-purine-9-yl]-*N*-methyl-β-D-ribofuranuronamide (IB-MECA). Results showed that melanoma cells highly expressed A3AR on the cell surface, which was rapidly internalized to the cytosol and "sorted" to the endosomes for recycling and to the lysosomes for degradation. Receptor distribution in the lysosomes was consistent with the down-regulation of receptor protein expression and was followed by mRNA and protein resynthesis. At each stage, receptor functionality was evidenced by the modulation in cAMP level and the downstream effectors protein kinase A, glycogen synthase kinase-3β, c-Myc, and cyclin D1. The A3AR antagonist MRS 1523 counteracted the internalization process as well as the modulation in the expression of the signaling proteins, demonstrating that the responses are A3AR-mediated. Supporting this notion are the *in vivo* studies showing tumor growth inhibition upon IB-MECA treatment and reverse of this response when IB-MECA was given in combination with MRS 1523. In addition, in melanoma tumor lesions derived from IB-MECA-treated mice, the expression level A3AR and the downstream key signaling proteins were modulated in the same pattern as was seen *in vitro*. Altogether, our observations tie the fate of A3AR to modulation of downstream molecular mechanisms leading to tumor growth inhibition both *in vitro* and *in vivo*.

The incidence of melanoma in humans has increased steadily over the past years and is one of the more difficult neoplasias to clinically manage. Due to the limited response of malignant melanoma to conventional chemotherapy and the poor prognosis of patients with metastatic melanoma, new therapies for this disease are needed.

Our earlier studies demonstrated that IB-MECA,[1] a stable agonist to A3AR, inhibits the proliferation of neoplastic cells including metastatic melanoma (1–3). A3AR belongs to the family of the G_i protein-associated cell surface receptors. Receptor activation leads to inhibition of adenylyl cyclase activity, cAMP formation, and PKA expression. PKA contains a catalytic subunit, PKAc, which dissociates from the parent molecule upon activation with cAMP, resulting in the initiation of various signaling pathways (4, 5). Recent studies have demonstrated that PKAc phosphorylates and inactivates GSK-3β (6). We showed that IB-MECA alters the expression of GSK-3β and β-catenin, key components of the Wnt signaling pathway. Consequently it led to inhibition in the expression of the cell cycle progression genes, c-Myc and cyclin D1 (2). This is an important observation as the Wnt pathway has been linked to the development of malignant melanoma (7–9).

It is well established that G_i protein receptors are internalized to early endosomes upon agonist binding. Early endosomes serve as the major site of receptor recycling, whereas the late endosomes are involved in the delivery of the internalized receptor to the lysosomes (10). One point to consider while targeting chronically a G_i protein receptor is that desensitization may lead to loss of a functional receptor from the cell surface.

Interestingly, although A3AR expression level was found to be low in most body tissues, it is highly expressed in tumor cell lines (11–13). Given that IB-MECA inhibits the growth of B16-F10 melanoma cells, it was hypothesized that these cells exhibit high receptor levels, which may serve as a target for tumor growth inhibition. We thus sought to explore the fate of A3AR upon IB-MECA activation and the consequences on the downstream molecular mechanisms leading to tumor growth inhibition both *in vitro* and *in vivo*.

Here we show that melanoma cells highly express A3AR, which upon IB-MECA stimulation rapidly internalizes to the cytosol and sorts to endosomes and lysosomes. Resynthesis and externalization of the receptor to the cell surface then occurs. Receptor functionality was demonstrated by the initiation of signal transduction pathways, which resulted in down-regulation of c-Myc and cyclin D1, leading to tumor growth suppression.

EXPERIMENTAL PROCEDURES

Reagents—IB-MECA and MRS 1523 were purchased from RBI/Sigma. For both reagents, a stock solution of 10 mM was prepared in Me_2SO, and further dilutions in RPMI medium were performed. RPMI, fetal bovine serum, and antibiotics for cell cultures were obtained from Beit Haemek, Haifa, Israel. ^{125}I-AB-MECA was purchased from Amer-

* The costs of publication of this article were defrayed in part by the payment of page charges. This article must therefore be hereby marked "*advertisement*" in accordance with 18 U.S.C. Section 1734 solely to indicate this fact.

¶ To whom correspondence should be addressed. Tel.: 972-3-9241114; Fax: 972-3-9249378; E-mail: pfishman@post.tau.ac.il.

[1] The abbreviations used are: IB-MECA, 1-deoxy-1-[6-[[(3-iodophenyl)methyl]amino]-9*H*-purine-9-yl]-*N*-methyl-β-D-ribofuranuronamide; AB-MECA, (*N*-6-(4-amino-3-iodobenzyl)-5′-*N*-methylcarbamoyladenosine; A3AR, A3 adenosine receptor; GSK-3β, glycogen synthase kinase-3β; PBS, phosphate-buffered saline; PKA, protein kinase A; PKB, protein kinase B; FITC, fluorescein isothiocyanate.

sham Biosciences. Rabbit polyclonal antibodies against murine and human A3AR, PKAc, c-Myc, and GSK-3β were purchased from Santa Cruz Biotechnology Inc., Santa Cruz, CA. Rabbit polyclonal antibodies against murine and human cyclin D1 were purchased from Upstate Biotechnology, Lake Placid, NY, and Cy3-conjugated anti-goat IgG and fluorescein-conjugated anti-rabbit IgG were purchased from Chemicon, Temecula, CA. FITC-dextran, FITC-transferrin, and forskolin were obtained from Sigma, and 8-Bromo-cAMP and MG132 were obtained from Calbiochem.

Immunostaining and Confocal Microscopy—B16-F10 murine melanoma cells were grown for 24 h on coverslips coated with poly(L-lysine) (500 μg/ml). Cells were incubated with IB-MECA (10 nM) or with IB-MECA + MRS 1523 (100 nM). To further show the immunostaining specificity, splenocytes derived from wild type C57Bl/6J mice or A3AR−/− mice (14) (kindly supplied by Marlene Jacobson from Merck Research Laboratories) were mounted on poly(L-lysine) slides for 3 h. Cells were fixed in 4% formaldehyde in phosphate-buffered saline (PBS) for 1 h at room temperature. The fixed cells were rinsed three times for 1 min with PBS. To block nonspecific interaction of the antibodies, cells were incubated for 30 min in 4% normal goat serum in PBS (1% bovine serum albumin, 0.1% Triton X-100). For A3AR labeling, cells were then incubated with the primary antibody against A3AR at a dilution of 1:1000 in PBS (1% bovine serum albumin, 1% normal goat serum, 0.1% Triton X-100) for 24 h at 4 °C. After being washed three times for 3 min with PBS, cells were incubated with Cy3-conjugated anti-goat IgG at a dilution of 1:250 in PBS and incubated in the dark for 2 h. Cells were rinsed with PBS three more times and mounted with AM 100 media (Chemicon). For the colocalization experiments, the endosomes were labeled by incubating cells with 200 μg/ml FITC-transferrin in media lacking serum for 60 min before incubating with IB-MECA (10 nM) for different time periods.

Lysosomes were labeled by incubating cells with 1 mg/ml FITC-dextran in RPMI with 1% serum at 37 °C for 24 h. Cells were washed with media and reincubated for an additional 1.5 h in media lacking serum following incubation with IB-MECA (10 nM) for different time periods. Cells were washed with PBS and fixed with 4% formaldehyde, and the A3AR was labeled as mentioned above. Stained cells were visualized by a confocal microscope (Zeiss, Axiovert 100 M, excitation at 553 and emission at 568 nm for Cy3, and at 492 and 520 nm, respectively, for fluorescein).

Measurement of cAMP Production—B16-F10 melanoma cells (1×10^6/ml) were serum-starved overnight and then incubated with IB-MECA. cAMP levels were determined under basal conditions and in cells challenged for 5, 15, and 30 min with forskolin (50 nM) in the presence or absence of IB-MECA (10 nM). Cells were lysed by the addition of 0.1 M HCl, and cell lysates were collected by centrifugation for 10 min at 1000 rpm. Dried samples were stored at −20 °C until used. For determination of cAMP production, a commercial enzyme-linked immunosorbent assay kit based on competitive protein binding method (R&D systems, Minneapolis, MN) was used. Four different experiments were performed.

^{125}I-AB-MECA Cell Surface Binding—To evaluate receptor surface density upon IB-MECA treatment, a radioligand binding assay was carried out in intact B16-F10 melanoma cells (see Ref. 20). Cells were serum-starved overnight, washed with PBS, and then incubated with IB-MECA (10 nM) for different time periods at 37 °C. At the end of the incubation period, cells were placed on ice and then rapidly washed three times with 120 mM NaCl, 5 mM KCl, 2 mM $CaCl_2$, 50 mM Tris, and 1 mM EDTA, pH 3.5 (acid T_1 buffer) (to remove the agonist). Cells were then incubated with 0.5 nM ^{125}I-AB-MECA in T_1 buffer at pH 8.12 at 4 °C for 120 min. The assay was performed in the absence or in the presence of 100 nM IB-MECA for nonspecific binding determination. This experiment was repeated three times.

Western Blot Analysis—To detect the level of expression of the desired proteins in B16-F10 melanoma cells, Western blot analysis was performed. Cells were serum-starved overnight and then incubated in the presence and absence of IB-MECA (10 nM), MRS 1523 (100 nM), forskolin (50 nM), or MG132 (20 nM) for different time periods at 37 °C with 1% fetal bovine serum. Cells were then rinsed with ice-cold PBS and transferred to ice-cold lysis buffer (TNN buffer, 50 mM Tris buffer, pH 7.5, 150 mM NaCl, Nonidet P-40 0.5% for 20 min). Cell debris was removed by centrifugation for 10 min at $7500 \times g$. The supernatant was utilized for Western blot analysis. Protein concentrations were determined using the Bio-Rad protein assay dye reagent. Equal amounts of the sample (50 μg) were separated by SDS-PAGE, using 12% polyacrylamide gels. The resolved proteins were then electroblotted onto nitrocellulose membranes (Schleicher & Schuell). Membranes were blocked with 1% bovine serum albumin and incubated with the desired primary antibody (dilution 1:1000) for 24 h at 4 °C.

To evaluate the specific binding, a blocking peptide corresponding to the peptide antigen (Santa Cruz Biotechnology) was used. Blots were then washed and incubated with a secondary antibody for 1 h at room temperature. Bands were recorded using 5-bromo-4-chloro-3-indolyl phosphate/nitro blue tetrazolium (BCIP/NBT) color development kit (Promega, Madison, WI). The optical density of the bands was quantified using an image analysis system and corrected by the optical density of the corresponding actin bands. Data presented in the different figures are representative of at least three different experiments.

Northern Blot Analysis—Total RNA was isolated from B16-F10 melanoma cells treated with IB-MECA (10 nM) or IB-MECA + MRS 1523 (100 nM) for 1 h, utilizing TRI reagent (Sigma). The samples were then subjected twice to phenol:chloroform extraction and washed with chloroform. RNA was precipitated with sodium acetate/ethanol following washing with ethanol, and then denatured, separated (25 μg/lane) in 1.1% formaldehyde agarose gel, and transferred to Hybond-N membrane. The 390-bp *Eco*RI fragment from A3AR cDNA clone of mouse (TAA3I.S), kindly supplied by Dr Kathia Ravid, was prepared by random-primed synthesis. Probes were used in RNA blot analysis at a hybridization temperature of 42 °C in the presence of 50% formamide.

In Vivo Studies—C57BL/6J, male mice (Harlan Laboratories, Jerusalem, Israel) aged 2 months, weighing an average of 25 g, were used. Mice were maintained on a standardized pelleted diet and supplied with tap water. Experiments were performed in accordance with the guidelines established by the Institutional Animal Care and Use Committee at the Rabin Medical Center, Petah Tikva, Israel.

The effect of IB-MECA on the development of subcutaneous tumors in C57Bl/6J mice was studied. B16-F10 (2.5×10^5) melanoma cells were subcutaneously injected to mice flank. Treatments as detailed below were administered orally twice daily, starting 24 h after the inoculation of the tumor cells. Four groups of mice were included in the study and treated as follows: 1) control, vehicle only; 2) IB-MECA, 10 μg/kg; 3) IB-MECA (10 μg/kg) + MRS 1523 (100 μg/kg); 4) MRS 1523, 100 μg/kg.

On day 15, the mice were treated with IB-MECA and sacrificed after 1 h. Tumor size (width (W) and length (L)) was measured with a caliper and calculated according to the following formula: tumor Size = $(W)^2 \times L/2$. Tumor lesions were then excised and homogenized (Polytron, KINEMATICA), and protein was extracted and subjected to Western blot analysis for the determination of A3AR. Each group contained 15 mice, and the study was repeated three times.

Statistical Analysis—The results were evaluated using the Student's t test, with statistical significance at $p < 0.05$. Comparison between the mean value of different experiments was carried out.

RESULTS

Localization of A3AR in B16-F10 Melanoma Cells—To study receptor localization, we utilized confocal laser microscopy. Untreated cells (control) highly exhibited A3AR on the cell surface, as seen from the fluorescence intensity level. A marked decrease in the fluorescence level was noted after 5 min in the IB-MECA-treated cells. Exposure of the melanoma cells to the antagonist MRS 1523 in the presence of IB-MECA resulted in cell surface fluorescence intensity similar to that of the control (Fig. 1*A*). These data suggest that rapid receptor internalization took place upon IB-MECA treatment. The specificity of receptor immunostaining was evidenced by showing marked fluorescence in splenocytes derived from wild type mice as compared with negative staining in splenocytes from A3AR knockout mice (Fig. 1*B*).

To further explore the time course kinetic of A3AR internalization, B16-F10 melanoma cells were exposed for different time periods to IB-MECA, and confocal microscopy analysis was carried out. Fig. 2 depicts the gradual internalization rate that occurred within a few minutes, resulting in the disappearance of the fluorescence after 6 min. Prolonged exposure (15 min) of the melanoma cells to IB-MECA resulted in receptor recycling to the cell surface. This was followed by internalization/recycling after longer incubation time periods (30 and 60 min). To confirm the observation that the fluorescence level is

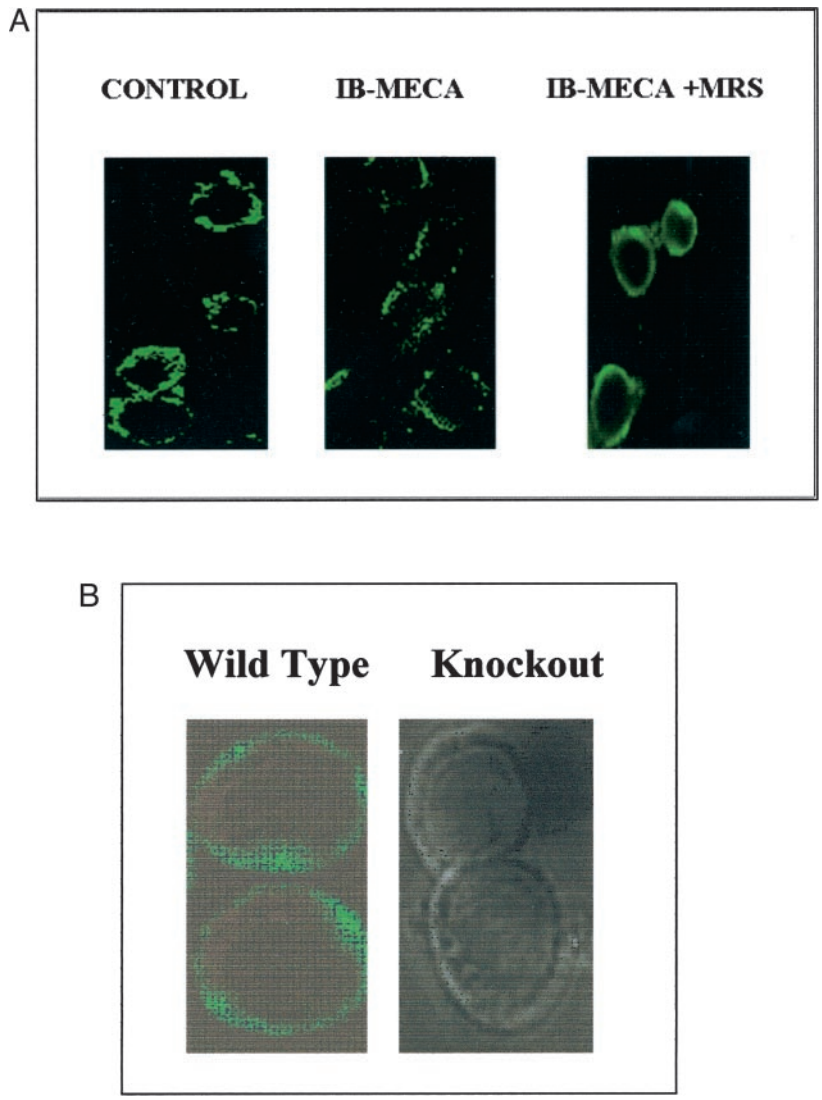

FIG. 1. **Melanoma cells highly exhibit A3AR, which is down-regulated upon IB-MECA treatment (confocal microscopy imaging).** B16-F10 melanoma cells were incubated for 5 min at 37 °C with 10 nM IB-MECA. The cells were labeled with the primary and secondary antibodies against A3AR and the Cy3-conjugated anti-goat IgG, respectively. Images represent the center section of the X-Y plane. *A*, exhibition of A3AR in melanoma cells. High fluorescence intensity is depicted in the control cells, whereas in IB-MECA-treated cells, lower fluorescence is seen. The combined treatment with IB-MECA and the antagonist MRS 1523 (100 nM) for 5 min results in fluorescence similar to that of the control. *B*, splenocytes derived from wild type mice (showing A3AR-positive staining) in comparison with splenocytes derived from A3AR knockout mice (negative staining).

decreased as a result of internalization, we performed optical sectioning of the cells. In untreated cells (control), the receptor was exhibited on the cell surface (Fig. 3, *upper left*), and upon exposure to IB-MECA for 5 min, it was presented inside the cell (Fig. 3, *upper right*), supporting the notion that A3AR translocates from the membrane to the cytosol. After 15 and 60 min, the receptor was accumulated in the cytosol (Fig. 3, *lower left* and *right*).

To assess differences in subcellular localization of A3AR following exposure to IB-MECA, we examined the time-dependent colocalization of A3AR with FITC-transferrin and FITC-dextran, known to accumulate in distinct subcellular compartments. Fig. 4*A* demonstrates that in unstimulated cells, the A3AR distribution (*green*) displays a membrane localization pattern, whereas transferrin (*red*) was accumulated in small vesicles. At 5 and 15 min after treatment with IB-MECA, a significant colocalization of A3AR and transferrin in the early endosomes was observed (colocalization shown in *yellow/orange*). However, when cells were exposed to IB-MECA for 60 min, less colocalization of A3AR and transferrin was evident (Fig. 4*A*). Time-dependent localization of A3AR with lysosomes (*red*) was revealed in cells labeled with FITC-dextran. Unstimulated cells displayed A3AR on the cell surface, and dextran was localized to large vesicles typical of lysosomes, many of which are centrally located in the cells (Fig. 4*B*, *upper left*). After 5 min of incubation with IB-MECA, some colocalization with dextran was observed. Following 15 min of exposure, A3AR exhibited significant increase in co-localization but was less evident at 60 min of incubation. Taken together, these results demonstrate that upon internalization, A3AR is transported to the early endosomes and to the lysosomes, suggesting that sequestration occurred mainly within the first 5 min of the exposure to IB-MECA, whereas the distribution to lysosomes occurred later, peaking at 15 min.

Radioligand Binding to Surface Receptor of IB-MECA-treated Cells—To evaluate receptor surface density, IB-MECA-treated cells were exposed to ^{125}I-AB-MECA for different time period. Fig. 5 shows that radioligand binding was decreased after 15 (55%) and 60 min (33%), demonstrating that IB-MECA induced accumulated internalization of A3AR. Interestingly, full recovery of the receptor to the cell surface was observed after 24 h.

RNA and Protein Expression Level of A3AR in IB-MECA-treated Melanoma Cells—Time-dependent expression of A3AR in the melanoma cells was examined by Western blot analysis. IB-MECA-induced modulation of A3AR expression in a sinusoidal pattern, *i.e.* down-regulation and up-regulation, occurred at different time points (Fig. 6*A*). When blocking peptide was utilized, the A3AR band disappeared, confirming that the 32-kDa band is A3AR-specific.

To test whether protein expression was modulated due to degradation and resynthesis, we exposed the cells for 1 h to

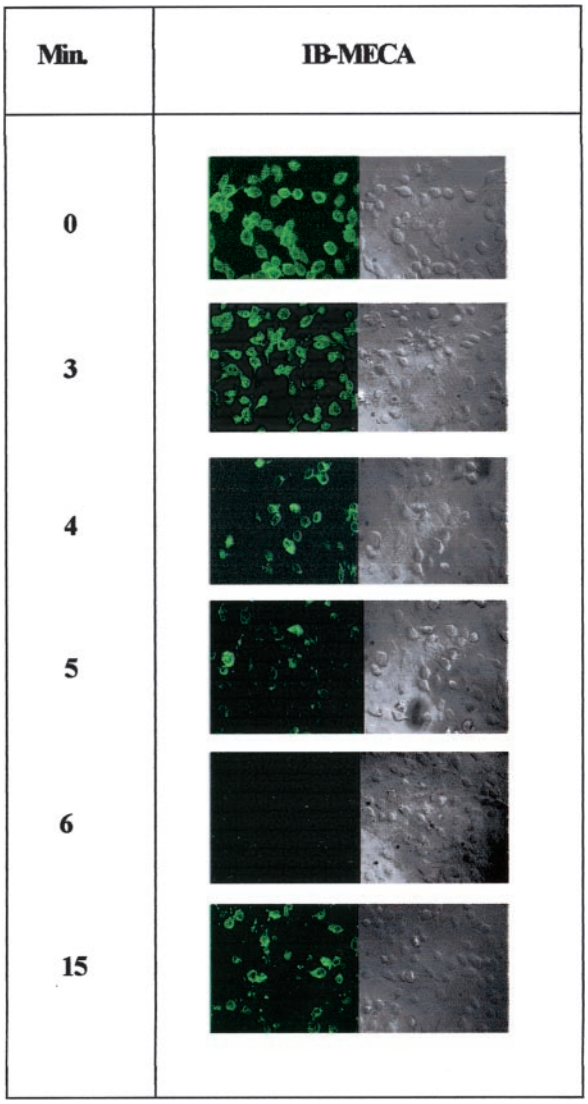

FIG. 2. **Time course of A3AR internalization/externalization in B16-F10 melanoma cells (confocal microscopy imaging).** B16-F10 melanoma cells were incubated for different time periods at 37 °C with 10 nM IB-MECA. Cells were labeled with the primary antibody against A3AR and the secondary antibody, Cy3-conjugated anti-goat IgG. Images represent the center section of the X-Y plane. Control cells exhibited high fluorescence, gradually disappearing upon IB-MECA treatment for 3, 4, and 6 min. Fluorescence was apparent again after 15 min, when the receptor was externalized to the cell surface.

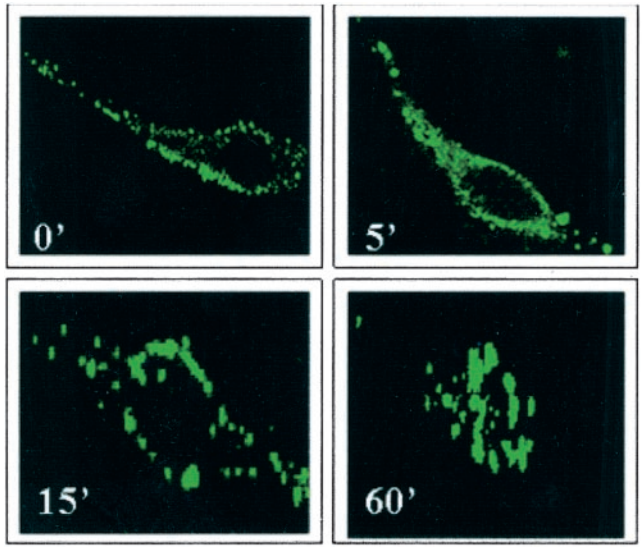

FIG. 3. **Time course of A3AR internalization/externalization in optical sections of B16-F10 melanoma cells (confocal microscopy imaging).** B16-F10 melanoma cells were incubated for different time periods at 37 °C with 10 nM IB-MECA. Cells were labeled with the primary antibody against A3AR and with the secondary antibody (Cy3-conjugated anti-goat IgG antibody). Images were acquired as single midcellular optical sections at 20 scans/frame. In untreated cells, green fluorescence labeling, representing A3AR, was confined to the cell surface. After 5 min of incubation, green labeling was distributed in the cytosol. At 15 min, the green labeling was less abundant, and at 60 min, green fluorescence was distributed throughout the cytosol and on the cell surface.

IB-MECA in the presence of MG132, a protein degradation inhibitor. Indeed, MG132 prevented A3AR down-regulation, illustrating that following internalization, receptor degradation took place (Fig. 6*B*). We next examined mRNA expression level upon exposure of the cells to IB-MECA for 1 h. Expression level was up-regulated, suggesting that resynthesis of A3AR had occurred (Fig. 6*C*). The specificity of this response was demonstrated by utilizing the selective antagonist MRS 1523, which reversed the increase in mRNA expression.

IB-MECA Modulates Key Elements Downstream to A3AR Activation—To show A3AR functionality in the B16-F10 melanoma cells, we tested cAMP production level and the protein expression level of the downstream effectors PKAc and GSK-3β (known from our former study to be up-regulated upon A3AR activation) (2). IB-MECA inhibited forskolin-stimulated cAMP accumulation after 5 and 15 min, whereas after 30 min, cAMP level was similar to that of the control value (Fig. 7*A*). Decreased PKAc and increased GSK-3β levels were observed after 15 min, whereas at 30 min, PKAc level stabilized, and GSK-3β only slightly increased (Fig. 7*B*). The specificity of this response was demonstrated by introducing forskolin to the culture system, which counteracted the effect of IB-MECA and prevented the modulation in PKAc and GSK-3β level (Fig. 7*C*). These results corroborated with the cAMP data, indicating that receptor desensitization/resensitization took place upon chronic exposure to the agonist.

To further evaluate the association between receptor activation, the subsequent downstream signaling events, and the specificity of these responses, B16-F10 melanoma cells were exposed to IB-MECA in the presence and absence of MRS 1523 for 15 min. PKAc and GSK-3β levels were modulated as was described above, leading to down-regulation in the expression level of cyclin D1 and *c-myc*, the two cell cycle progression genes. MRS 1523 antagonized the modulation in the expression level of the proteins, indicating that the response was mediated via the A3AR (Fig. 8).

IB-MECA Inhibits Melanoma Development in Mice—IB-MECA markedly suppressed the development of B16-F10 melanoma tumor growth in the flank model (52% inhibition, $p < 0.0001$, Fig. 9*A*). In mice treated with a combination of IB-MECA and MRS 1523, no inhibition was noted, demonstrating that the antagonist counteracted the activity of IB-MECA and that the response was A3AR-mediated. In tumor lesions excised from these mice, Western blot analysis revealed down-regulation of A3AR, c-Myc, and cyclin D1 and up-regulation of GSK-3β expression level (Fig. 9*B*). This modulation in the level of proteins was also neutralized by MRS 1523, further demonstrating the specificity of the response.

DISCUSSION

IB-MECA is a synthetic A3AR agonist exhibiting a potent antiproliferative effect against tumor cells both *in vitro* and *in vivo* (1, 2, 15, 16). In this study, we show that B16-F10 mela-

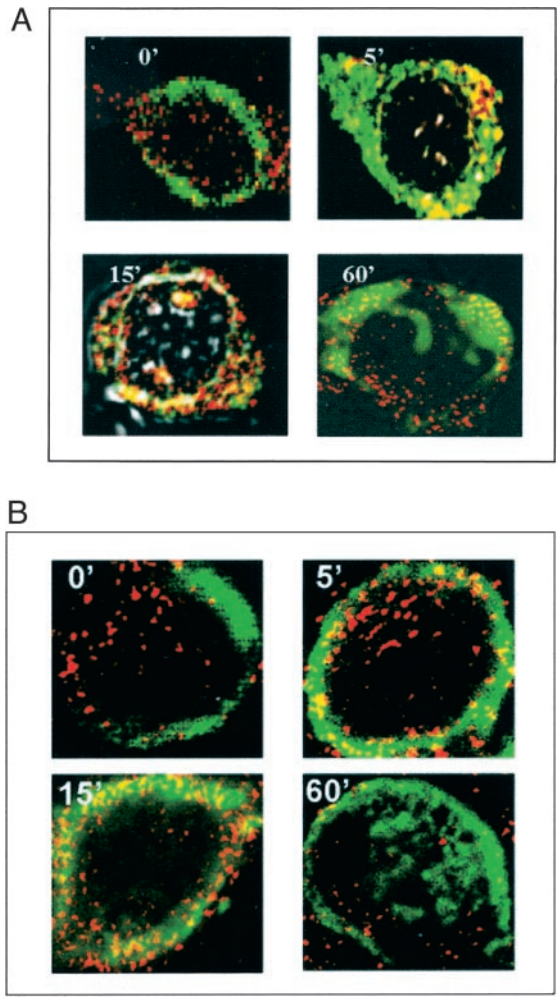

FIG. 4. **Time course of A3AR colocalization with transferrin and dextran in B16-F10 melanoma cells exposed to IB-MECA (confocal microscopy imaging).** In *A*, to tag the endosomes, melanoma cells were labeled with 200 μg/ml FITC-transferrin (*red*) in media without serum for 60 min in the presence and absence of IB-MECA (10 nM) for different time periods. The A3AR was labeled as mentioned above (*green*). In *B*, lysosomes were labeled by incubating cells with 1 mg/ml FITC-dextran (*red*) in RPMI with 1% serum at 37 °C for 24 h. Cells were washed and reincubated for an additional 1.5 h in media lacking serum following incubation with IB-MECA (10 nM) for different time periods. The A3AR was labeled as mentioned above (*green*). For both *A* and *B*, stained cells were visualized by a confocal microscope (Zeiss, Axiovert 100 M, excitation at 553 and emission at 568 nm for Cy3, and at 492 and 520 nm, respectively, for fluorescein).

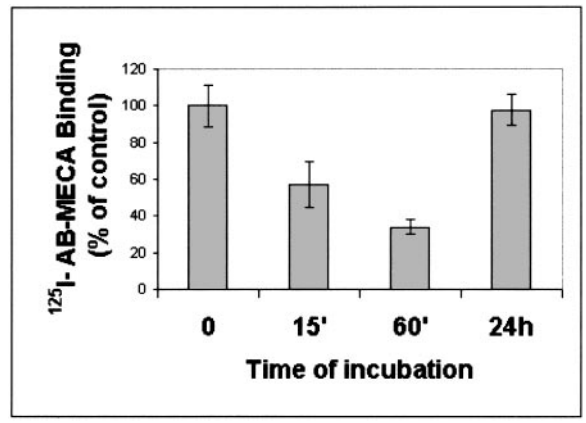

FIG. 5. **Cell surface A3AR density in IB-MECA-treated cells as evaluated by ^{125}I-AB-MECA binding assay.** B16-F10 melanoma cells were incubated for different time periods at 37 °C with 10 nM IB-MECA. After incubation, cells were washed to remove agonist. Cell surface A3AR density was evaluated by measuring the radioligand binding at 4 °C for 120 min. Data, expressed as percent of control, represent values of three different experiments.

noma cells highly express A3AR. Exposure of the receptor to IB-MECA resulted in receptor internalization/externalization followed by the modulation of key proteins involved in signaling pathways leading to tumor growth inhibition.

Four experimental approaches to test A3AR exhibition and expression in B16-F10 melanoma cells were used in this study. In confocal microscopy analysis, the exhibition of A3AR on the cell surface was exemplified by massive fluorescence, which disappeared on IB-MECA treatment, later to reappear, indicating that receptor internalization/recycling had taken place. The specificity of this response was proved by the introduction of the antagonist MRS 1523 to the culture system in the presence of IB-MECA, resulting in cell surface receptor exhibition similar to the control. The antagonist blocked ligand binding, preventing internalization, thereby retaining full receptor exhibition. Supporting the internalization/externalization event are the studies in which confocal microscopy sectioning exemplified the translocation of the receptor from the membrane to the cytosol. Furthermore, the radioligand binding assay showed accumulated decrease in surface receptor density upon IB-MECA treatment and full recovery of the receptor to the cell surface after 24 h. Tagging the cells with transferrin confirmed the assumption that the receptor was internalized. Transferrin primarily internalizes with transferrin receptors and constitutively recycles with the receptors through early endosomes to a recycling compartment and then back to the cell surface (10, 17). Our data showing colocalization of A3AR with transferrin after 5 and 15 min, both in the cytoplasm and on the cell surface, support the notion that internalization followed by recycling took place. Taken together, it seems that based on the radioligand binding and the confocal microscopy data, a partial receptor recycling occurs after short incubation period, whereas full recovery takes place after a long period of time. This conclusion may suggest that part of the internalized receptor is subjected to degradation and that a subsequent receptor resynthesis is needed for full receptor recovery. Indeed, the high level of receptor expression was down-regulated shortly after IB-MECA treatment. Prolonged incubation periods resulted in repeated down-regulation/up-regulation of receptor expression, suggesting that this pattern may be a result of receptor degradation and resynthesis. To confirm this notion, we utilized MG132 that prevented receptor down-regulation due to its protease inhibitory effect. Additional data to support the view that part of the internalized receptor was degraded came from confocal microscopy studies in which the cells were labeled with FITC-dextran, which has been shown to specifically accumulate in lysosomes (18). Moreover, the increased expression level of protein and mRNA after 60 min of incubation indicated the involvement of both transcriptional and post-transcriptional events in the process of receptor resynthesis. Others also demonstrated A3AR internalization/recycling; however, the time course did not overlap our values, most probably due to the utilization of different cell types and agonist concentration (19–21).

Receptor functionality was tested by monitoring the level of cAMP and key proteins modulated upon A3AR activation. A decrease in PKAc and an increase in GSK-3β levels were observed both *in vitro* and *in vivo*. The modulation in the level of these proteins was antagonized by forskolin and MRS 1523. Interestingly, after a longer incubation period (30 min), receptor desensitization occurred and was manifested by reversing levels of PKAc and GSK-3β. In a previous study (2), we showed

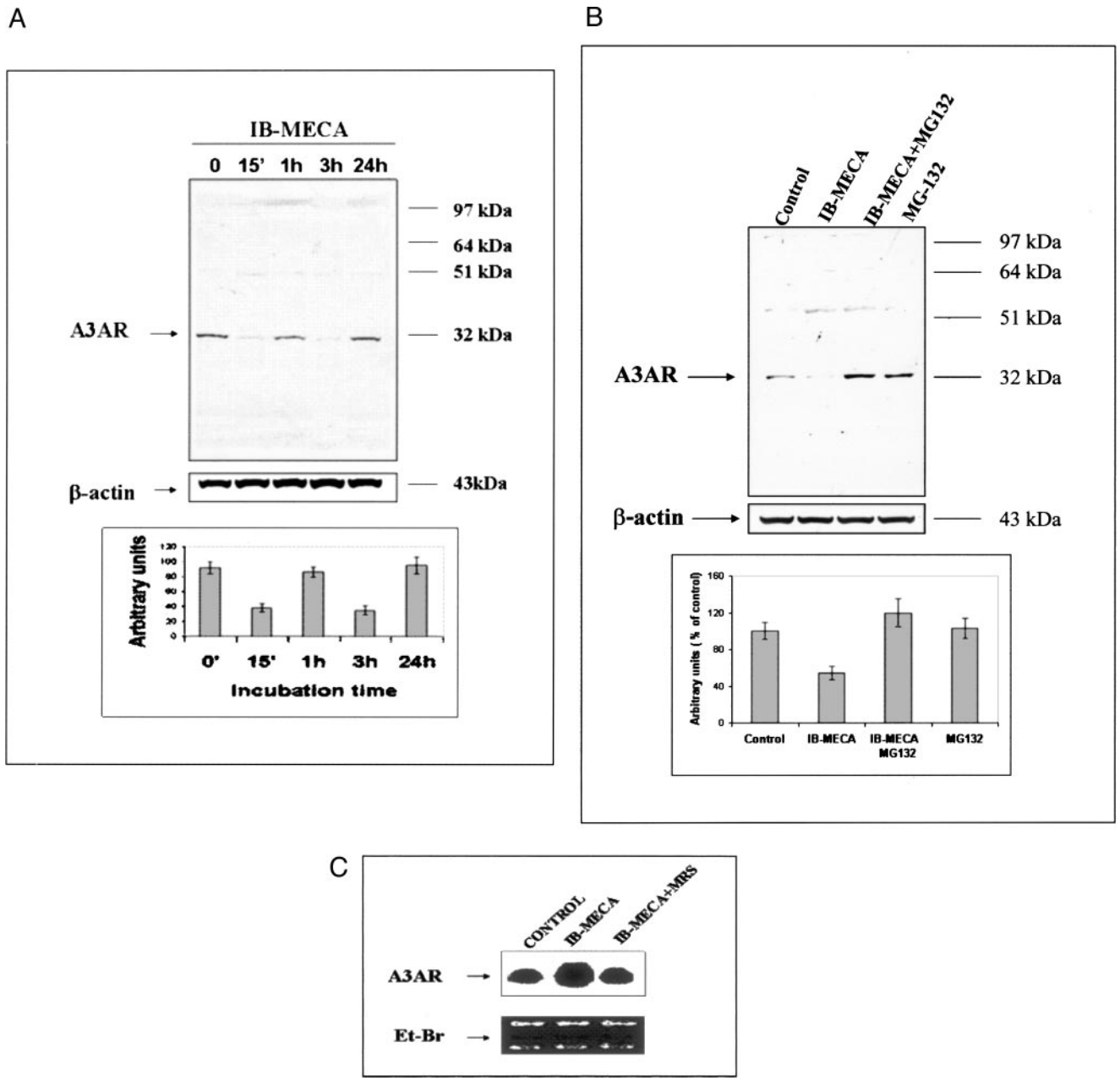

FIG. 6. **Protein and mRNA expression level of A3AR upon exposure to chronic IB-MECA treatment.** B16-F10 melanoma cells were incubated for different time periods at 37 °C with 10 nM IB-MECA. For *A* and *B*, blots were probed with antibodies against A3AR. In *A*, A3AR expression is down-/up-regulated during chronic activation by 10 nM IB-MECA In *B*, after 15 min of incubation with IB-MECA, the proteasome inhibitor MG132 prevented A3AR degradation (*lane 3*). *C*, Northern blot analysis of A3AR mRNA extracted from control (*lane 1*), cells treated with IB-MECA for 1 h (*lane 2*), cells treated with IB-MECA + MRS 1523 for 1 h (*lane 3*).

that IB-MECA inhibited melanoma cell growth via cross-talk between A3AR and the Wnt signaling pathway. A3AR activation was found to inhibit PKAc and PKB, thereby retaining GSK-3β in its active nonphosphorylated form (2). GSK-3β was shown to phosphorylate and inactivate β-catenin, which consequently induced the down-regulation of c-Myc and cyclin D1 (22). In some tumor cells, including melanoma, GSK-3β fails to phosphorylate β-catenin, which accumulates in the cytosol. It then translocates to the nucleus, where it induces the transcription of cyclin D1 and *c-myc*, leading to cell cycle progression (7–9). It thus seems that signal transduction pathways initiated upon receptor sensitization also need to be turned off (desensitized) to ensure that signaling can be achieved, allowing the regulation of cell function. Receptor desensitization led to signal termination despite the continuous presence of the agonist in the culture system. Subsequent resensitization, *i.e.* the expression of a functional receptor on the cell surface being capable of generating signaling pathways, took place. This chain of events is typical in other G-protein-coupled receptors (23, 24).

Remarkably, IB-MECA was also efficacious in suppressing melanoma development in mice. The expression profile of A3AR and GSK-3β, in the tumor lesions derived from IB-MECA-treated mice, was similar to that shown *in vitro*. Moreover, cyclin D1 and c-Myc levels were down-regulated in the melanoma lesions. These two cell cycle progression genes have been reported earlier to be overexpressed in melanoma cells (25, 26). This suggests their down-regulation as part of the mechanism of melanoma growth inhibition by IB-MECA.

The specificity of tumor suppressive response to IB-MECA

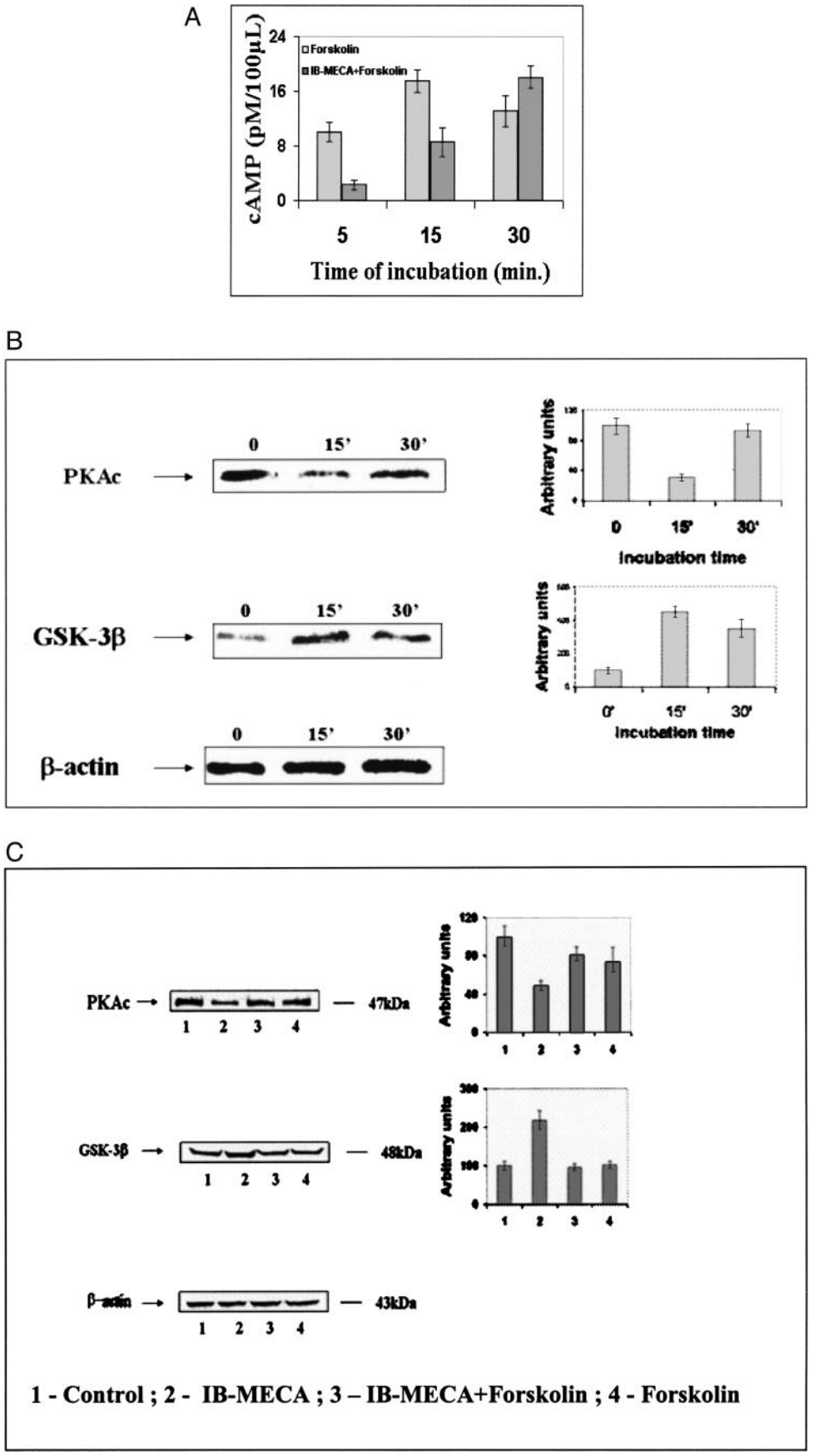

FIG. 7. **Receptor functionality is demonstrated by monitoring the level of key elements downstream to A3AR activation.** *A*, effect of IB-MECA (10 nM) on forskolin-stimulated cAMP production. *B*, immunoblots showing the effect of 10 nM IB-MECA on the expression level of PKAc and GSK-3β in B16-F10 melanoma cells at different time points. *C*, cells treated (15 min) simultaneously with IB-MECA + forskolin.

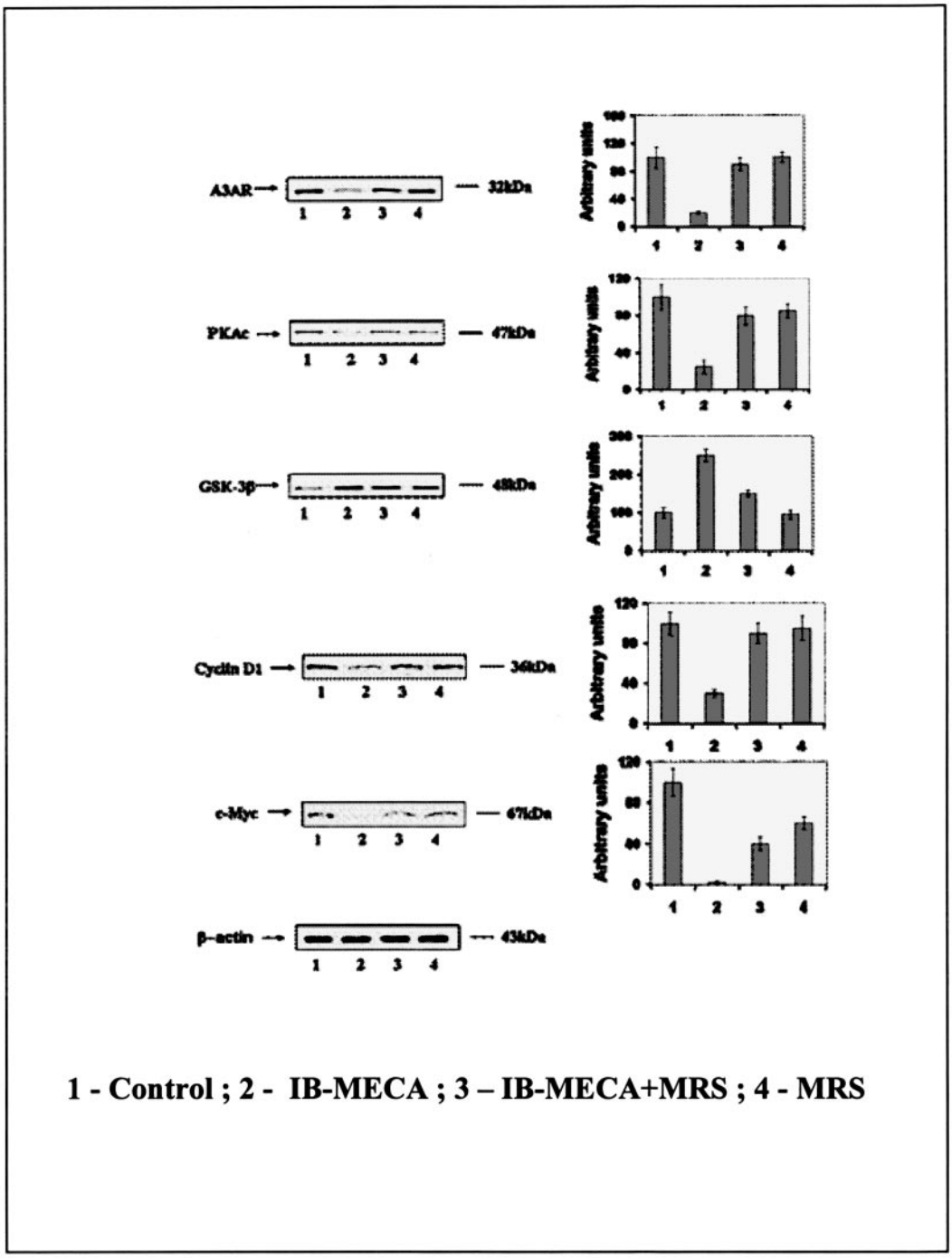

FIG. 8. **Modulation of cell growth regulatory proteins in B16-F10 melanoma cells upon IB-MECA treatment.** This figure displays immunoblots showing the effect of 10 nM IB-MECA on the expression level of A3AR, PKAc, GSK-3β, c-Myc, and cyclin D1 in B16-F10 melanoma cells. Serum-starved cells (for 18 h) were treated for 15 min with IB-MECA in the presence of 1% fetal bovine serum. To test the specificity of these responses, the antagonist MRS 1523 (100 nM) was introduced to the culture system.

was confirmed *in vivo* when melanoma-bearing mice were treated with IB-MECA + MRS 1523. The latter blocked most of the inhibitory effect of IB-MECA, demonstrating that the response is A3AR-mediated. Earlier studies demonstrated that A3AR agonists such as IB-MECA or Cl-IB-MECA, at micromolar concentrations, induced apoptosis in different cell types. In some of the studies, the activity was found to be A3AR-mediated, whereas in others, A3AR antagonists did not counteract the effect, demonstrating that the apoptosis was not A3AR-mediated (27, 28). In distinction from these studies, in the present work, IB-MECA was used at nanomolar concentrations, and its activity was counteracted by the antagonist MRS 1523, demonstrating that the response was A3AR-dependent.

In conclusion, melanoma cells highly express and exhibit A3AR. Upon activation, the receptor is internalized to the cytosol, "sorted" to the early endosomes, and recycled to the cell surface. Alternatively, the receptor may be targeted to lysosomes and then subjected to degradation followed by resynthesis and externalization. Modulation of key proteins leading to tumor growth inhibition both *in vitro* and *in vivo* was demonstrated.

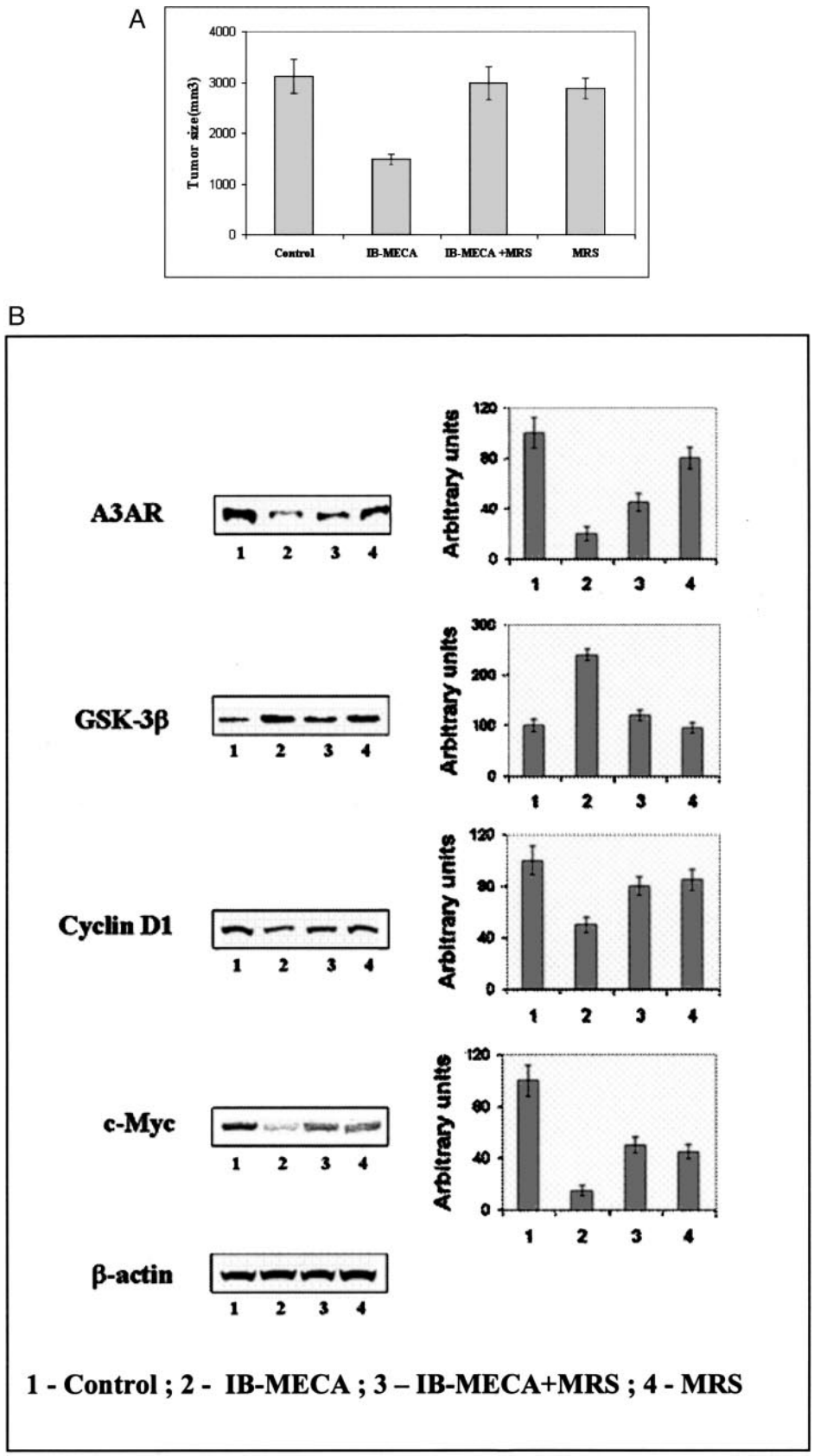

FIG. 9. **Inhibition of melanoma cell growth in mice and modulation of cell growth regulatory proteins in tumor lesions.** B16-F10 melanoma cells were subcutaneously inoculated to mice and then treated daily with IB-MECA (10 μg/kg) or IB-MECA in combination with MRS 1523 (100 μg/kg). On day 15, tumor size was measured, and 1 h after IB-MECA treatment, tumor lesions were excised, and then protein was extracted and subjected to Western blot analysis. *A*, tumor size in the different treated groups (15 mice in each group). IB-MECA inhibited the development of lung metastatic foci ($p < 0.0001$). The antagonist MRS 1523 counteracted the effect of IB-MECA ($p < 0.005$). *B*, immunoblots showing the effect of IB-MECA and MRS 1523 on A3AR, GSK-3β, cyclin D1, and c-Myc expression level in protein extracts derived from the melanoma tumor lesions.

REFERENCES

1. Fishman, P., Bar-Yehuda, S., Ohana, G., Pathak, S., Wasserman, L., Barer, F., and Multani, A. S. (2001) *Exp. Cell Res.* **269,** 230–236
2. Fishman, P., Madi, L., Bar-Yehuda, S., Barer, F., Del Valle, L., and Khalili, K. (2002) *Oncogene* **21,** 4060–4064
3. Ohana, G., Bar-Yehuda, S., Barer, F., and Fishman, P. (2001) *J. Cell. Physiol.* **186,** 19–23
4. Olah, M. E., and Stiles, G. L. (2000) *Pharmacol. Ther.* **85,** 55–75
5. Poulsen, S. A., and Quinn, R. J. (1998) *Bioorg. Med. Chem.* **6,** 619–641
6. Fang, X., Yu, S. X., Lu, Y., Bast, R. C., Woodgett, J. R., and Mills, G. B. (2000) *Proc. Natl. Acad. Sci. U. S. A.* **97,** 11960–11965
7. Robbins, P. F., El-Gamil, M., Li, Y. F., Kawakami, Y., Loftus, D., Appella, E., and Rosenberg, S. A. (1996) *J. Exp. Med.* **183,** 1185–1192
8. Morin, P. J. (1999) *BioEssays* **21,** 1021–1030
9. Bonvini, P., Hwang, S. G., El-Gamil, M., Robbins, P., Kim, J. S., Trepel, J., and Neckers, L. (2000) *Biochim. Biophys. Acta* **1495,** 308–318
10. Schmid, S. L., Fuchs, R., Male, P., and Mellman, I. (1988) *Cell* **52,** 73–83
11. Gessi, S., Varani, K., Merighi, S., Morreli, A., Ferrari, D., Leung, E., Baraldi, P. G., Spalutto, G., and Borea, P. A. (2001) *Br. J. Pharmacol.* **134,** 116–126
12. Merighi, S., Varani, K., Gessi, S., Cattabriga, E., Iannotta, V., Ulouglul, C., Leung, E., and Borea, P. A. (2001) *Br. J. Pharmacol.* **134,** 1215–1226
13. Suh, B. C., Kim, T. D., Lee, J. U., Seong, J. K., and Kim, K. T. (2001) *Br. J. Pharmacol.* **134,** 132–142
14. Montesinos, M. C., Desai, A., Delano, D., Chen, J. F., Fink, J. S., Jacobson, M. A., and Cronstein, B. N. (2003) *Arthritis Rheum.* **48,** 240–247
15. Merimsky, O., Madi, L., Bar-Yehuda, S., and Fishman, P. (2003) *Drug Dev. Res.* **58,** 386–389
16. Fishman, P., and Bar-Yehuda, S. (2003) *Curr. Top. Med. Chem.* **3,** 1349–1364
17. Ceresa, B. P., and Schmid, S. L. (2000) *Curr. Opin. Cell Biol.* **12,** 204–210
18. Petrou, C., Chen, L., and Tashjian, A. H., Jr. (1997) *J. Biol. Chem.* **272,** 2326–2333
19. Trincavelli, M. L., Tuscano, D., Cecchetti, P., Falleni, A., Benzi, L., Klotz, K. N., Gremigni, V., Cattabeni, F., Luccachini, A., and Martini, C. (2000) *J. Neurochem.,* **75,** 1493–1501
20. Trincavelli, M. L., Tuscano, D., Marroni, M., Falleni, A., Gremigni, V., Ceruti, S., Abbracchio, M. P., Jacobson, K. A., Cattabeni, F., and Martini, C. (2002) *Mol. Pharmacol.* **62,** 1373–1384
21. Ferguson, G., Watterson, K. R., and Palmer, T. M. (2002) *Biochemistry* **41,** 14748–14761
22. Ferkey, D. M., and Kimelman, D. (2000) *Dev. Biol.* **225,** 471–479
23. Bunemann, M., Lee, K. B., Pals-Rylaasdam, R., and Hosey, M. (1999) *Annu. Rev. Physiol.* **61,** 169–192
24. Claing, A., Laporte, S. A., Caron, M. G., and Lefkowitz, R. J. (2002) *Prog. Neurobiol.* **66,** 61–79
25. D'agnano, I., Valentini, A., Fornari, C., Bucci, B., Starace, G., Felsani, A., and Citro, G. (2001) *Oncogene* **20,** 2814–2825
26. Parrella, P., Caballero, O. L., Sidranski, D., and Merbs, S. L. (2001) *Investig. Ophthalmol. Vis. Sci.* **42,** 1679–1688
27. Kim, S. G., Ravi, G., Hoffmann, C., Jung, Y. J., Kim, M., Chen, A., and Jacobson, K. A. (2002) *Biochem. Pharmacol.* **63,** 871–880
28. Appel, E., Kazimirsky, G., Ashkenazi, E., Kim, S. G., Jacobson, K. A., and Brodie, C. (2001) *J. Mol. Neurosci.* **17,** 285–292